Lattice Dynamics and Phase Transitions of Strontium Titanate

R. A. COWLEY*
Crystallographic Laboratory, Cavendish Laboratory, Cambridge, England
(Received 16 December 1963)

The crystal dynamics of strontium titanate has been studied both experimentally and theoretically. The frequency versus wave-vector dispersion curves for some of the normal modes propagating along the [0,0,1] direction have been measured by neutron spectrometry at 90 and 296°K. The experiments were performed at the Chalk River Laboratories of Atomic Energy of Canada Ltd., using a triple-axis crystal spectrometer. The temperature dependence of the transverse optic mode of the lowest frequency has been found to be in agreement with the temperature dependence of the dielectric constant, as predicted by Cochran. The experimental results have been used to obtain the parameters of several models, more than one of which gives reasonable agreement with the experimental results. It is suggested that the anomalous behavior of the elastic properties and the phase transition at 110°K are associated with an accidental degeneracy of two branches of the dispersion curves; the longitudinal acoustic branch and the transverse optic branch of lowest frequency. The origin of the temperature dependence of this transverse optic mode and the relevance of lattice dynamics to the phase transitions in other perovskites are discussed.

I. INTRODUCTION

THE lattice dynamics of strontium titanate has been studied both theoretically and experimentally, in an attempt to understand the lattice dynamics of a ferroelectric material. Anderson[1] and Cochran[2] have independently suggested that the anomalous temperature dependence of the static dielectric constant of ferroelectrics is associated with the temperature dependence of a transverse optic mode of vibration. Recently, this low-frequency mode of vibration has been observed experimentally in barium and strontium titanates, by using infrared spectrometry[3,4] and in strontium titanate by using neutron spectrometry.[5]

In this paper experimental measurements are presented of some of the frequency versus wave-vector dispersion curves for normal modes propagating in the [0,0,1] direction of strontium titanate. These dispersion curves were determined by neutron spectrometry using the triple-axis crystal spectrometer[6] at the N.R.U. reactor at the Chalk River Laboratories of Atomic Energy of Canada Limited.

The simplest model which is used to describe the lattice dynamics of ionic crystals is the rigid-ion model.[7,8] In this model the ions interact with one another through both long-range electrostatic forces and short-range repulsive forces between neighboring ions. This model has been shown to be inadequate to describe the measured dispersion curves of two alkali halides, sodium iodide[9,10] and potassium bromide.[10] These experimental results showed that a more satisfactory model was the shell model,[9] which takes account of the polarizability of the ions in both electrostatic and short-range forces.

The experimental measurements on strontium titanate have been used to obtain the parameters of both rigid-ion models and shell models. These parameters show that it is possible to obtain the large changes in the frequency of the lowest transverse optic mode by changing the values of the parameters only slightly.

Recently, it has been found that the ultrasonic attenuation in strontium titanate increases dramatically below 110°K, while the elastic constants show an anomalous temperature dependence.[11,12] A possible explanation for these observations is put forward in terms of an instability of the crystal arising from the accidental degeneracy of two branches of the dispersion curves. Finally the results are discussed with particular reference to the origin of ferroelectricity in the perovskite structure.

II. THEORY OF THE LATTICE DYNAMICS OF STRONTIUM TITANATE

1. Symmetry

Some of the properties of the normal modes of vibration of a crystal are a direct consequence of its symmetry. The degeneracies between the different branches of the dispersion curves, and the separation of the normal modes into longitudinal and transverse vibrations for some wave vectors are examples of these properties. For simple crystals these relations can be obtained by inspection, but for more complicated crys-

* Visitor at Atomic Energy of Canada Limited, 1961–62, where some of the work described below was done.

[1] P. W. Anderson, Izd.AN. SSR., Moscow (1960).

[2] W. Cochran, Advan. Phys. **9**, 387 (1960).

[3] A. S. Barker and M. Tinkham, Phys. Rev. **125**, 1527 (1962).

[4] W. G. Spitzer, R. C. Miller, D. A. Kleinman, and L. E. Howarth, Phys. Rev. **126**, 1710 (1960).

[5] R. A. Cowley, Phys. Rev. Letters **9**, 159 (1962).

[6] B. N. Brockhouse, *Inelastic Scattering of Neutrons in Solids and Liquids* (International Atomic Energy Agency, Vienna, 1961), p. 113.

[7] E. W. Kellermann, Phil. Trans. Roy. Soc. **A238**, 513 (1940).

[8] M. Born and K. Huang, *Dynamical Theory of Crystal Lattices* (Oxford University Press, London, 1954).

[9] A. D. B. Woods, W. Cochran, and B. N. Brockhouse, Phys. Rev. **119**, 980 (1960).

[10] A. D. B. Woods, B. N. Brockhouse, R. A. Cowley, and W. Cochran, Phys. Rev. **131**, 1025 (1963).

[11] R. O. Bell and G. Rupprecht, Phys. Rev. **129**, 90 (1963).

[12] K. S. Krogstad and R. W. Moss, Bull. Am. Phys. Soc. **7**, 192 (1962).

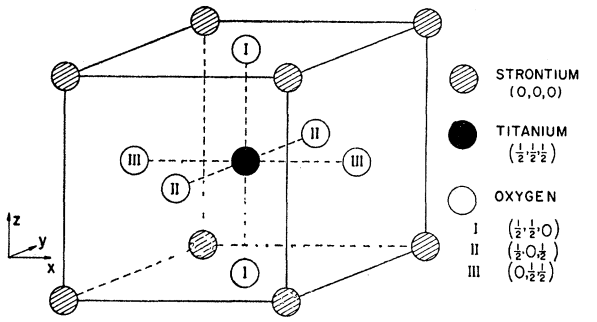

FIG. 1. The crystal structure of strontium titanate.

tals a more systematic procedure is given by using group theory.[13]

The normal modes of vibration are classified by assigning them to an irreducible representation of the space group of the crystal. A representation for the normal modes is obtained by choosing as a set of basis vectors the displacement of each ion in turn along a coordinate axis. If the character of a symmetry operation S is $\chi(S)$ in this representation, and its character in the λ irreducible representation is $\chi^\lambda(S)$, then

$$\chi(S)=\sum_\lambda C_\lambda \chi^\lambda(S), \qquad (1)$$

where C_λ is the number of times the λ irreducible representation occurs in the original representation.

When the normal modes of the crystal are described by Bloch waves, the irreducible representations of the symmorphic space groups can be obtained from the irreducible representations of the little group, which is that point group which leaves the wave vector unchanged. The irreducible representations are then obtained from Eq. (1) and from the characters of the irreducible representations of the point groups.[13,14]

The structure of strontium titanate is cubic perovskite, and the space group is $Pm3m$. The ions are situated on five interpenetrating simple cubic lattices as shown and labeled in Fig. 1. The characters of the different symmetry elements in the original representation are listed in Appendix I.

(a) $\zeta=(0,0,0)$

The little group is $m3m$, and the irreducible representations are

$$4\Gamma_{15}+\Gamma_{25}.$$

This result is, however, incorrect because the effect of the macroscopic electric field has been neglected. This electric field splits the degeneracy of some of the normal modes because the boundary conditions for the longitudinal and transverse modes differ.[8] The degeneracies will be lifted for those normal modes which transform like an ordinary vector. Since an ordinary vector transforms like Γ_{15}, the degeneracies associated with three of the four irreducible representations Γ_{15} are split. The fourth irreducible representation corresponds to a uniform translation of the whole crystal. There are, therefore, the three acoustic modes, $\omega=0$, a triply degenerate normal mode Γ_{25}, and three longitudinal and doubly degenerate transverse optical modes.

(b) $\zeta=(0,0,\zeta)$

The little group is $4mm$, and the irreducible representations are

$$4\Delta_1+\Delta_2+5\Delta_5.$$

The normal modes Δ_1 and Δ_2 are longitudinally polarized modes, while those represented by Δ_5 are doubly degenerate transverse modes.

At the zone boundary the little group is $4/mmm$, and the irreducible representations are

$$2M_1+2M_2'+M_3+3M_5+2M_5'.$$

M_5 and M_5' correspond to doubly degenerate transverse modes, while the other modes are longitudinally polarized.

(c) $\zeta=(\zeta,\zeta,0)$

The little group is mm except at the zone boundary, where it is $4/mmm$. The irreducible representations are

$$5\Sigma_1+\Sigma_2+5\Sigma_3+4\Sigma_4,$$

and

$$M_1+M_2+M_2'+M_3+2M_3'+M_4+M_5+3M_5'.$$

There are no degeneracies at general points, but at the zone boundary there are four doubly degenerate normal modes.

(d) $\zeta=(\zeta,\zeta,\zeta)$

The little group at a general point is $3m$ and its irreducible representations are

$$4\Lambda_1+\Lambda_2+5\Lambda_3.$$

At the zone boundary the little group symmetry is increased to $m3m$ and the irreducible representations are

$$\Gamma_2'+\Gamma_{12}'+\Gamma_{25}+\Gamma_{25}'+2\Gamma_{15}.$$

The irreducible representation Λ_3 corresponds to doubly degenerate normal modes, while at the zone boundary there are four triply degenerate normal modes, one doubly degenerate pair and a single normal mode.

2. Models

In the last section we found the properties of the normal modes which can be deduced from the symmetry of the crystal. In order to evaluate the frequencies of any of the normal modes, a particular model must be

[13] V. Heine, *Group Theory in Quantum Mechanics* (Pergamon Press, Inc., New York, 1960).
[14] G. F. Koster, *Solid State Physics*, edited by F. Seitz and D. Turnbull (Academic Press Inc., New York, 1957), Vol. V.

employed for the interactions between the ions. The simplest model which has been used for ionic crystals is the rigid-ion model.[7,8] The equation of motion for this model is then written in the harmonic approximation as

$$M_K\omega^2\mathbf{U}(K)=\sum_{K'}(\mathbf{R}_{KK'}+Z_K\mathbf{C}_{KK'}Z_{K'})\mathbf{U}(K'), \quad (2)$$

where the notation is the same as that of Woods *et al.*[9]

This model does not satisfactorily account for the dispersion curves of the alkali halides,[9,10] because it neglects the polarizabilities of the ions. These polarizabilities can be introduced by using the shell model.[2,9] The equations of motion of the shell model in the harmonic approximation[9] are

$$\begin{aligned} M_K\omega^2\mathbf{U}(K)&=\sum_{K'}(\mathbf{R}_{KK'}+Z_K\mathbf{C}_{KK'}Z_{K'})\mathbf{U}(K') \\ &\quad+\sum_{K'}(\mathbf{T}_{KK'}+Z_K\mathbf{C}_{KK'}Y_{K'})\mathbf{W}(K'), \\ 0&=\sum_{K'}(\mathbf{T}_{K'K}+Y_K\mathbf{C}_{KK'}Z_{K'})\mathbf{U}(K') \\ &\quad+\sum_{K'}(\mathbf{S}_{KK'}+Y_K\mathbf{C}_{KK'}Y_{K'})\mathbf{W}(K'). \end{aligned} \quad (3)$$

The matrices $\mathbf{T}_{KK'}$ and $\mathbf{S}_{KK'}$ give the short-range interactions between the displacements and the electronic dipole moments, and between the electronic dipole moments, respectively. In general, the elements $\mathbf{R}_{KK'}$, $\mathbf{T}_{KK'}$ and $\mathbf{S}_{KK'}$ are all different and must be specified by different short-range force constants. However the shell charges Y_K can be chosen so that $\mathbf{R}_{KK'}=\mathbf{T}_{KK'}$ when the wave vector is zero,[15] and it was further assumed that they are then equal for all wave vectors. The validity of this approximation and the further approximation that $\mathbf{S}_{KK'}=\mathbf{R}_{KK'}+\mathbf{k}_K\delta_{KK'}$ are discussed by Cowley, Cochran, Woods, and Brockhouse.[15] The model then corresponds to a shell model in which all the short-range forces act through the shells.

In actual calculations the short-range forces were assumed to be axially symmetric. If the equilibrium condition is imposed then these forces become central forces and the elastic constants obey Cauchy's relation, $C_{12}=C_{44}$. In practice, this relation is nearly satisfied, but the equilibrium condition was not imposed on the models described below.

For each type of short-range interaction two parameters are needed to specify axially symmetric forces. These parameters were chosen to be the derivatives of a potential function parallel and perpendicular to the line joining the interacting ions. These were defined in a similar way to those used for the alkali halides.[7,9,15]

The forces were specified by

$$\left(\frac{\partial^2V}{\partial r^2}\right)_{\parallel}=\frac{e^2A_i}{2v}, \quad \left(\frac{\partial^2V}{\partial r^2}\right)_{\perp}=\frac{e^2B_i}{2v},$$

where the suffix i is one for strontium-oxygen, two for titanium-oxygen, and three for oxygen-oxygen forces. Each type of force was assumed to act only between nearest neighbors. The short-range contributions to the dynamical matrix were then evaluated by the usual procedure,[8] and the elements are listed in Appendix II.

The ionic charges were specified by two charges; that on the strontium ion was Z_1e and on the titanium ion Z_2e. The charge on the oxygen ion is then $Z_3e=-\frac{1}{3}(Z_1+Z_2)e$.

The polarizabilities of the ions were specified in a similar way to that used for the alkali halides.[9,15] These polarizability parameters were chosen so that they were independent of the choice of the shell charges. The electrical polarizability was defined as

$$\alpha_i=Y_i^2/[k_i+(T_{ii})_0],$$

and the short-range polarizability as

$$d_i=-Y_i(T_{ii})_0/[k_i+(T_{ii})_0],$$

where the suffix i has values 1 for the strontium ion, 2 for the titanium and 3 for the oxygen, and $(T_{11})_0=2A_1+4B_1$, $(T_{22})_0=A_2+2B_2$. The oxygen-ion polarizabilities are not isotropic, so that the polarizability was defined in terms of a mean $(T_{33})_0$ given by,

$$(T_{33})_0=\tfrac{1}{3}(2A_1+4B_1+A_2+2B_2+4A_3+8B_3).$$

The most complicated rigid-ion model of the crystal, then, has eight adjustable parameters, six for the short-range forces and two for the ionic charges, while for a shell model there are fourteen parameters, the same eight and six polarizability parameters.

3. Calculation of Dielectric and Elastic Constants

The frequencies of the normal modes of vibration can be obtained by solving Eq. (2) for a rigid-ion model, or Eqs. (3) for a shell model. Once a particular set of parameters has been chosen, their solution is quite straightforward when the electrostatic coupling coefficients are known. These coefficients were calculated using the EDSAC II computer at the Cambridge University Mathematical Laboratory, and their values for the (0,0,1) direction have already been reported.[16] These and the coefficients for the (1,1,0) and (1,1,1) directions are listed in Appendix III.

The dielectric constants can be evaluated in terms of the parameters introduced above.[2,17] The high-frequency dielectric constant is given by Eq. (2.44) of Ref. 17 and the static dielectric constant by Eq. (2.34). In practice the high-frequency dielectric constant was evaluated explicitly and the static dielectric constant obtained from the Lyddane-Sachs-Teller relation as extended by Cochran.[2]

[15] R. A. Cowley, W. Cochran, A. D. B. Woods, and B. N. Brockhouse, Phys. Rev. **131**, 1030 (1963).

[16] R. A. Cowley, Acta Cryst. **15**, 687 (1962).

[17] R. A. Cowley, Proc. Roy. Soc. (London) **A268**, 121 (1962).

The elastic constants were evaluated explicitly using the method of long waves as developed by Born and Huang[8] and Cowley.[17] Since every ion is situated at a center of symmetry, the polarizabilities do not affect the elastic constants. The electrostatic contributions were evaluated numerically.[16] The elastic constants are given by:

$$C_{11}=(2e^2/vr)[\tfrac{1}{8}(2A_1+2B_1+A_2+2A_3+2B_3)+0.16485(Z_1^2+Z_2^2)-0.78348Z_3^2-1.0721Z_1Z_2+2.67981Z_2Z_3-1.27803Z_1Z_3],$$

$$C_{12}=(2e^2/vr)[\tfrac{1}{8}(A_1-5B_1-B_2+A_3-5B_3)-0.55532(Z_1^2+Z_2^2)-1.60946Z_3^2+0.26873Z_1Z_2-1.43585Z_2Z_3+0.05648Z_1Z_3],$$

$$C_{44}=(2e^2/vr)[\tfrac{1}{8}(A_1+3B_1+B_2+A_3+3B_3)-0.08242(Z_1^2+Z_2^2)+0.39174Z_3^2+0.53605Z_1Z_2-1.33991Z_2Z_3+0.63902Z_1Z_3].$$

The electrostatic cohesive energy is $(e^2/r)\alpha_M$, where α_M, the Madelung constant, is given by

$$1.25950(Z_1^2+Z_2^2)+4.57109Z_3^2+0.79260Z_1Z_3-0.667170Z_2Z_3+0.48362Z_1Z_2.$$

The equilibrium condition is then

$$4\alpha_M+12(B_1+B_3)+3B_2=0.$$

This last equation when substituted into the equation for C_{12} gives $C_{12}=C_{44}$. r is half the lattice parameter and v the volume of the unit cell, $v=8r^3$.

III. THE EXPERIMENTS

1. Experimental Methods

The excellent single crystal of strontium titanate was a 150-carat boule provided by the Titanium Division of the National Lead Company. The mosaic spread was measured against that of a silicon crystal and was 0.25 deg. The crystal, which had [1,0,0] aligned along the length of the boule, was mounted in a metal cryostat, and could be either cooled or heated from above. It was aligned *in situ* by using neutrons.

The experiments were carried out by using a triple-axis crystal spectrometer.[6]

The integrated intensity of a neutron group, obtained using the "constant **Q**" technique,[6] is given in the harmonic approximation by[9]

$$\sigma=\frac{\hbar}{8\pi^2}\frac{|\mathbf{k}'|}{|\mathbf{k}_0|}\frac{H(\mathbf{q}j)^2}{\omega(\mathbf{q}j)}\begin{Bmatrix}N(\mathbf{q}j)\\N(\mathbf{q}j)+1\end{Bmatrix}.$$

$H(\mathbf{q}j)$ is the structure factor for the mode and is given by

$$H(\mathbf{q}j)=|\sum_K \exp(2\pi i\boldsymbol{\tau}\cdot\mathbf{R}(0K))\mathbf{Q}\cdot\mathbf{e}(K,\mathbf{q}j)b_K M_K^{-1/2}\times\exp(-W(K))|.$$

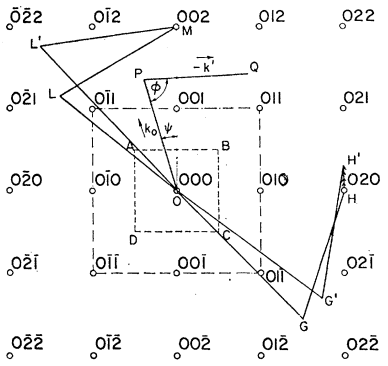

FIG. 2. The (1,0,0) plane of the reciprocal lattice of strontium titanate. The Brillouin zone is labeled ABCD and the area in which the reduced structure factor repeats is enclosed by (0,1,1), (0,1,$\bar{1}$), (0,$\bar{1}$,1) and (0,$\bar{1}$,$\bar{1}$). OLM and OL'M demonstrate the "constant-Q" technique in which the spectrometer is controlled so as to keep the momentum transfer constant while varying the energy transfer, while OGH and OG'H' shows the constant-energy technique in which the momentum is kept along the desired direction.

If a normal mode is propagating along the [0,0,1] direction then the motion of all the ions is either transverse or longitudinal. The dependence of the structure factor on the wave-vector transfer can then be separated out if we assume the Debye-Waller factors for the different atoms to be equal. We can then introduce a reduced structure factor for the normal mode

$$h(\mathbf{q}j)=|\sum_K \exp(2\pi i\boldsymbol{\tau}\cdot\mathbf{R}(0K))e(K,\mathbf{q}j)M_K^{-1/2}b_K|.$$

This reduced structure factor is periodic in reciprocal space. Figure 2 shows the (1,0,0) plane of the reciprocal lattice of strontium titanate. The Brillouin zone is labeled as ABCD, while the reduced-structure factor repeats over a larger unit in reciprocal space, enclosed on Fig. 2 by the reciprocal lattice points (0,$\bar{1}$,1), (0,1,1), (0,1,$\bar{1}$), and (0,$\bar{1}$,$\bar{1}$). Because the structure factor repeats over a larger volume in reciprocal space than the frequencies, there are several different points in reciprocal space at which phonons of the same wave vector have different reduced-structure factors. In the (1,0,0) plane there are four corresponding to reciprocal-lattice vectors, $\boldsymbol{\tau}$: (0,0,0), (0,1,0), (0,0,1) and (0,1,1).

The reduced-structure factor squared has been calculated for each of these different positions for normal modes propagating in the (0,0,1) direction, by using model IV of Sec. IV. The results are shown in Fig. 3.

2. Measurements of the Dispersion Curves

Measurements have been made at 90°K of four of the transverse branches and of most of three of the longitudinal branches. The measured branches are those with the lower frequencies. The results are illustrated in Figs. 7 and 9, where they are compared with several of the models described in the next section. The highest frequency transverse optic branch and the two highest

frequency longitudinal optic branches were not measured because of the extra difficulty in measuring these high frequencies. Unfortunately it was not possible to complete the measurements on the longitudinal acoustic branch with the crystal in the (1,0,0) plane.

Less complete measurements were made of three of the transverse branches and the longitudinal acoustic branch at 296°K. The results are shown in Figs. 7 and 9, where they are compared with calculations using several of the models described in the next section.

The frequencies of the normal modes with long wavelength, $\mathbf{q}=0$, can also be obtained by using infrared spectroscopy. Strontium titanate has been studied by Last,[18] Barker and Tinkham[3] and by Spitzer *et al.*[4] The frequencies of the transverse modes can be obtained directly from these measurements, and those of the longitudinal modes by using a result due to Kurosawa,[19] as explained by Cochran and Cowley.[20] In Table I the results of the infrared and neutron techniques are listed, for the $\mathbf{q}=0$ modes.

Since in strontium titanate each ion is situated at a center of symmetry, its Raman spectrum is a second-order spectrum and depends upon the joint density of states for the phonons. Narayanan and Vedam[21] have erroneously interpreted their results as a first-order spectrum.

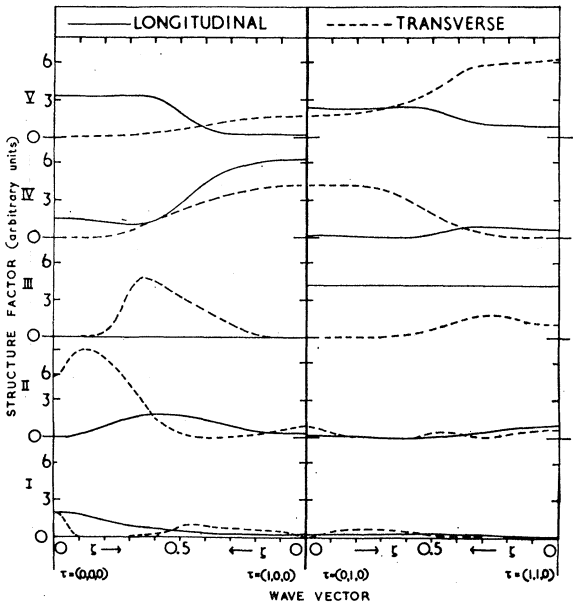

FIG. 3. The reduced structure factor for normal modes propagating along the $(\zeta,0,0)$ direction calculated using model IV of Sec. IV. The solid lines show longitudinal modes and the transverse modes are polarized along the y direction and shown by dotted lines. The modes are labeled in order of increasing frequency.

[18] J. T. Last, Phys. Rev. **105**, 1740 (1957).
[19] T. Kurosawa, J. Phys. Soc. Japan **16**, 1298 (1961).
[20] W. Cochran and R. A. Cowley, *Inelastic Scattering of Slow Neutrons* (International Atomic Energy Agency, Vienna, 1963), Vol. I.
[21] P. S. Narayanan and K. Vedam, Z. Physik **163**, 158 (1961).

TABLE I. The frequencies of the $\mathbf{q}=0$ optical modes in strontium titanate (units; 10^{12} c/sec) as determined by neutron and infrared spectrometry. The measurements with an asterisk are at 90°K and the others at 296°K.

Normal mode	Neutron spectroscopy measurements	Infrared measurements (3)	(4)
Transverse			
ν_1	1.27*	1.20*	...
	2.73	3.00	2.63
ν_2	5.10*	...	5.34
ν_3	7.95*	...	...
ν_4	...	16.5	16.3
Longitudinal			
ν_1	5.10*	...	5.25
ν_2	7.95*	...	...
ν_3	...	14.5	13.8
ν_4	...	24.5	24.9

3. The Temperature Dependence of the Lowest Frequency Transverse Optic Mode

Cochran[2] has shown that, if the static dielectric constant of a crystal follows a Curie law temperature dependence,

$$\epsilon^0=C/(T-T_c), \tag{4}$$

the temperature dependence of the $\mathbf{q}=0$ transverse optic mode with lowest frequency is expected to be

$$\omega_T^2=K(T-T_c). \tag{5}$$

Mitsui and Westphal[22] and Weaver[23] have shown that the static dielectric constant above 70°K follows a Curie Law with a Curie temperature of about 35°K.

The $\mathbf{q}=0$ mode of the transverse optic branch with lowest frequency has been studied at five different temperatures, and the neutron groups obtained at three of these temperatures are shown in Fig. 4. The increase in intensity on the low-frequency side of the 90°K group is due to the elastic and acoustic mode scattering associated with the (0,2,0) reciprocal lattice point. The asymmetry of some of the groups and the change in the width of the neutron groups with temperature are probably largely due to effects associated with the finite resolution of the spectrometer.

Figure 5 shows a plot of the frequencies squared against temperature for this normal mode. The excellent straight line gives ample evidence for Eq. (5), and the validity of discussing ferroelectrics as a problem in lattice dynamics, as suggested by Cochran.[2] The Curie temperature is given by the intercept of the straight line with the temperature axis, which yields a Curie temperature of 32 ± 5°K, which is in excellent agreement with the dielectric constant measurements.[22,23]

[22] T. Mitsui and W. B. Westphal, Phys. Rev. **124**, 354 (1961).
[23] H. E. Weaver, Phys. Chem. Solids **11**, 274 (1959).

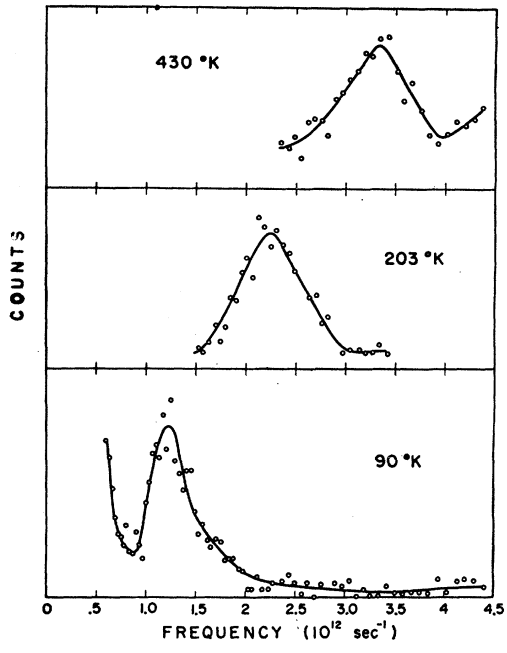

FIG. 4. Neutron groups for the $\mathbf{q}=0$ lowest frequency transverse optic mode at three different temperatures.

4. The Temperature Dependence of the Transverse Acoustic Branch

Recent measurements of the elastic constants of strontium titanate[11,12] have shown that on cooling from room temperature, C_{44} at first increases, but near 110°K it decreases quite dramatically.[11]

Neutron measurements have been made of the $\zeta=(0,0,0.2)$ transverse acoustic mode to see if a similar temperature dependence is found at these higher frequencies. The results are shown in Fig. 6 and there is clearly no evidence for any discontinuity at 110°K, within the limits of experimental error.

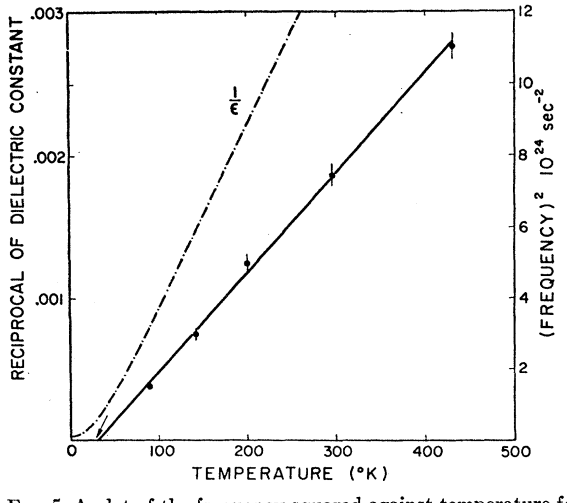

FIG. 5. A plot of the frequency squared against temperature for the $\mathbf{q}=0$ lowest frequency transverse optic mode. The dotted line shows the reciprocal of the static dielectric constant (Refs. 22 and 23).

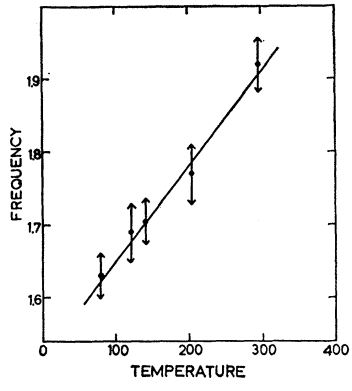

FIG. 6. A plot of the frequency (10^{12} c/sec) against temperature (°K) for the $\zeta=(0.2,0,0)$ transverse acoustic mode.

The ultrasonic measurements also showed anomalous attenuation below 110°K, but no anomalous broadening of the neutron groups at 90°K was detected for either the longitudinal or transverse acoustic branches.

IV. MODELS

The theory of the lattice dynamics of strontium titanate was described in Sec. II. In this section we discuss the results obtained when the parameters of these models are fitted to the experimentally measured elastic[24] and dielectric constants,[22,23,25] and to the fre-

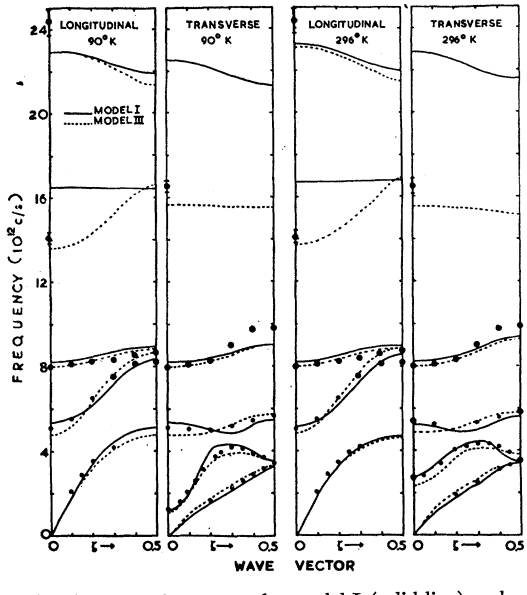

FIG. 7. The dispersion curves for model I (solid line) and model III (dotted line) for the normal modes propagating along the $(\zeta,0,0)$ direction. The experimental measurements are taken from both neutron and infrared results. (See Refs. 3 and 4.) The irreducible representations at the zone boundary are for the longitudinal modes M_2', M_1, M_3, M_1, M_2' in order of increasing frequency, while for the transverse modes they are M_5, M_5', M_5, M_5', M_5 (model I) and M_5', M_5, M_5, M_5', M_5 (model III).

[24] E. Poindexter and A. A. Giardini, Phys. Rev. **110**, 1069 (1958).

[25] S. B. Levin, N. J. Field, F. M. Plock, and L. Merker, J. Opt. Soc. Am. **45**, 737 (1955).

TABLE II. The parameters of the models described in Sec. IV. Those parameters which were varied in each model are given with the errors of the parameters, while for those which were kept fixed there are not any errors.

	Short-range forces $e^2/2v$						Ionic charge (e)	
	Strontium-Oxygen		Titanium-Oxygen		Oxygen-Oxygen		Strontium	Titanium
Model	A_1	B_1	A_2	B_2	A_3	B_3	Z_1	Z_2
90°K								
I	9.0±4.7	2.5±2.1	110.4±18.7	−36.6± 5.7	24.8±6.9	1.0±1.5	1.40±0.21	2.20±0.36
II	26.5±2.1	−2.0±1.3	288.5±10.3	−42.7± 2.4	−3.7±4.3	−0.1±0.9	2	4
III	26.9±2.5	−3.8±1.3	292.2±10.7	−41.4± 5.4	−6.8±5.0	0.8±1.2	2	4
IV	12.9±7.4	0.3±1.5	313.7±19.7	−64.0±18.0	5.3±8.8	0.4±3.9	1.26±0.47	4.64±0.16
V	6.9±1.5	2.6±0.9	321.4± 9.8	−70.1± 4.8	8.8±2.9	−2.1±0.7	0.83±0.07	4.94±0.08
VI	6.5±0.7	2.8±0.4	317.7± 2.4	−68.8± 0.7	9.8±0.6	−2.5±0.3	0.82625	4.9123
296°K								
I	2.9±2.3	6.7±4.6	112.1±20.9	−36.3± 6.5	28.3±7.7	0±1.8	1.20±0.16	2.32±0.35
II	27.6±2.8	−2.8±1.7	289.6±12.9	−39.2± 4.2	−2.9±5.4	−1.1±1.4	2	4
III	28.7±3.2	−4.2±2.0	293.3±12.0	−40.8± 9.2	−5.5±6.2	0.1±1.4	2	4
IV	16.5±7.0	−1.4±2.3	300.5±36.2	−46.1±14.8	5.5±8.6	−1.6±2.8	1.34±0.50	4.39±0.50
V	8.6±2.1	2.1±1.3	315.0±12.5	−70.2± 5.3	9.1±3.9	−2.3±0.9	0.83±0.07	4.91±0.09

	Polarizability (10^{-24}) cm^3 or (e)						Expected error of an observable/ exptl. error
	Strontium ion		Titanium ion		Oxygen ion		
Model	α_1	d_1	α_2	d_2	α_3	d_3	
90°K							
I	0	0	0	0	0	0	4.1
II	0.025	0	0.003	0	0.028±0.002	0.69±0.11	2.6
III	0.025	−0.35±0.29	0.003	−0.08±0.15	0.030±0.002	0.68±0.13	2.5
IV	0.025	−0.29±0.59	0.003	0.01±0.06	0.027±0.004	0.82±0.11	2.3
V	0.025	0	0.068±0.011	−2.13±0.46	0.018±0.003	0.51±0.14	1.7
VI	0.025	0	0.79441	−2.596	0.01535	0.42162	1.6
296°K							
I	0	0	0	0	0	0	4.4
II	0.025	0	0.003	0	0.028±0.004	0.68±0.15	3.3
III	0.025	−0.48±0.23	0.003	−0.05±0.16	0.029±0.003	0.69±0.15	2.8
IV	0.025	−0.18±0.53	0.003	0.03±0.09	0.027±0.003	0.78±0.16	2.7
V	0.025	0	0.079±0.011	−2.60±0.41	0.015±0.005	0.42±0.17	1.9

quencies of the normal modes as measured by infrared[3,4] and neutron spectrometry, as described in the last section. The fitting was performed by a nonlinear least-squares analysis and the numerical work was done using the EDSAC II computer.

Results have been obtained for several models at both 90 and 296°K. The parameters of these models are listed in Table II, while their agreement with the experimental elastic and dielectric constants is shown in Table III. The agreement with the measured dispersion relations is shown for models I and III in Fig. 7 and for models IV and V in Fig. 9. The dispersion relations in the (1,1,0) and (1,1,1) directions have also been calculated for some of the models and are shown in Figs. 8 and 10.

A particularly interesting feature of the models is that the large charges in the frequencies of the transverse optic mode with lowest frequency have been obtained with comparatively small changes in the parameters of the models. Model VI, for example, has the ionic charges and polarizabilities of model V at 296°K but fits the 90°K measurements with only small changes in the short-range force constants.

TABLE III. The agreement between the experimental elastic and dielectric constants and those calculated using the models.

	Elastic constants 10^{12} dynes cm^{-2}			Dielectric constants	
Model	C_{11}	C_{12}	C_{44}	ϵ^0	ϵ^∞
90°K					
Exptl.	3.35[a]	1.05[a]	1.27[a]	1305[b]	5.5[c]
I	2.95	1.00	1.01	193.1	1
II	3.26	1.07	1.80	1161.3	3.88
III	3.19	1.07	1.71	1171.8	3.83
IV	3.40	1.05	1.57	889.9	3.64
V	3.48	1.02	1.33	1227.4	5.66
VI	3.49	1.05	1.33	1150.7	6.30
296°K					
Exptl.	3.30[d]	1.01[d]	1.24[d]	301.0[b]	5.5[c]
I	2.98	1.12	1.02	37.9	1
II	3.30	1.25	1.80	300.9	3.8
III	3.31	1.27	1.71	292.9	3.8
IV	3.45	1.24	1.65	215.1	3.73
V	3.46	1.19	1.28	244.2	5.78

[a] These have been obtained from Eq. (8) neglecting the effects of the 110°K transition.
[b] See Refs. 22 and 23.
[c] See Ref. 25.
[d] See Ref. 11

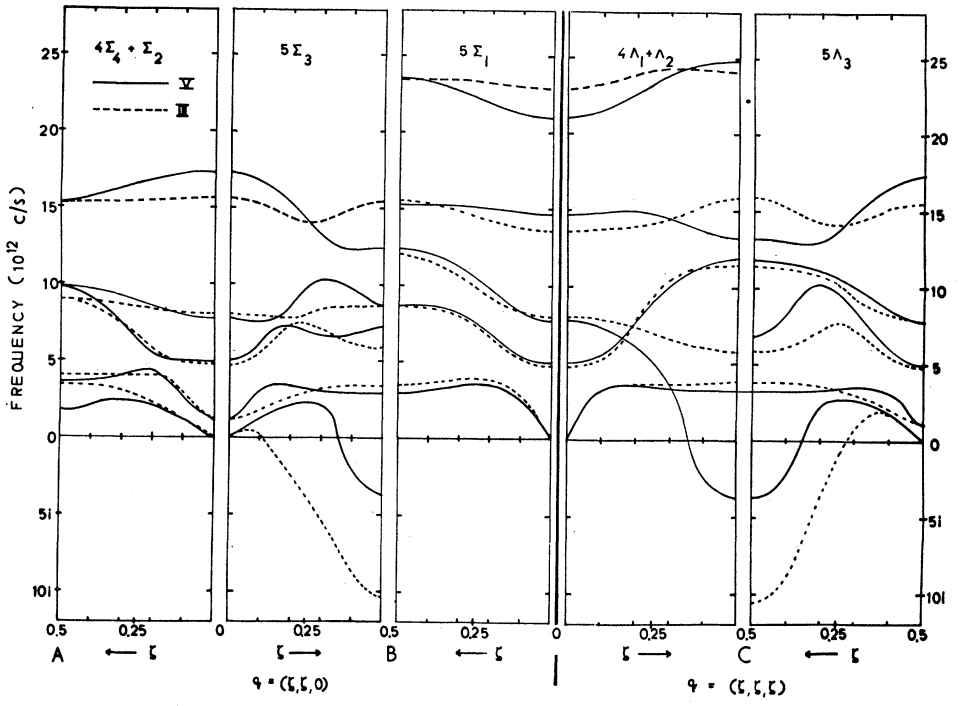

FIG. 8. The dispersion curves in the $(\zeta,\zeta,0)$ and (ζ,ζ,ζ) directions for models III and V at 90°K. The irreducible representations in order of increasing frequency are at the point (A); M_2', M_3', M_5, M_3' (model III), and M_3', M_2', M_5, M_3' (model V). At the point (B) they are M_2, M_5', M_3, M_5', M_1, M_5', M_4 for model III and M_3, M_5', M_2, M_5', M_5', M_1, M_4 for model V, while at the zone boundary (C) they are Γ_{12}', Γ_{15}, Γ_{25}, Γ_{15}, Γ_{25}', Γ_2' (model III), and Γ_{25}, Γ_{15}, Γ_{12}', Γ_{25}', Γ_{15}, Γ_2' (model V).

V. THE 110°K PHASE TRANSITION

1. The Temperature Dependence of the Elastic Constants

The temperature dependence of the elastic constants of crystals has been discussed by several authors.[8,26] The potential energy of the crystal is expanded in a double power series of the deformation parameters and of the phonon coordinates, Eq. (40.4) of Ref. 8.

If this expansion is taken about the equilibrium configuration of the lattice at each temperature, then the isothermal elastic constants can be obtained from[8,26]

$$(\alpha\beta,\gamma\delta)=\Phi_{\alpha\beta\gamma\delta}(--)+\sum_{\mathbf{q}}\sum_{j}\Phi_{\alpha\beta\gamma\delta}(--,\mathbf{q}j-\mathbf{q}j)(\hbar/2(\mathbf{q}j))(2n(\mathbf{q}j)+1)+\sum_{jj'}{}'\sum_{\mathbf{q}}\Phi_{\alpha\beta}(-,\mathbf{q}j-\mathbf{q}j')$$
$$\times\Phi_{\gamma\delta}(-,-\mathbf{q}j\mathbf{q}j')\frac{\hbar}{2\omega(\mathbf{q}j)}\left(\frac{2n(\mathbf{q}j)+1}{\omega^2(\mathbf{q}j)-\omega^2(\mathbf{q}j')}\right)-\sum_{j}\sum_{\mathbf{q}}\Phi_{\alpha\beta}(-,\mathbf{q}j-\mathbf{q}j)\Phi_{\gamma\delta}(-,\mathbf{q}j-\mathbf{q}j)$$
$$\times\left[\frac{\hbar}{4\omega(\mathbf{q}j)^3}(2n(\mathbf{q}j)+1)+\frac{\hbar^2}{2\omega(\mathbf{q}j)^2kT}n(\mathbf{q}j)(n(\mathbf{q}j)+1)\right]. \quad (6)$$

The notation is similar to that of Born and Huang.[8] The elastic constants are then given by

$$C_{\alpha\beta\gamma\delta}{}^{\mathrm{iso}}=(1/4V)[(\alpha\beta,\gamma\delta)+(\alpha\beta,\delta\gamma)+(\beta\alpha,\gamma\delta)+(\beta\alpha,\delta\gamma)].$$

The adiabatic and isothermal elastic constants are related by macroscopic relations, which in Voigt's notation are

$$C_{11}{}^{\mathrm{ad}}-C_{11}{}^{\mathrm{iso}}=C_{12}{}^{\mathrm{ad}}-C_{12}{}^{\mathrm{iso}}$$
$$=(TV\alpha^2/C_V)(C_{11}{}^{\mathrm{iso}}+2C_{12}{}^{\mathrm{iso}})^2,$$
$$C_{44}{}^{\mathrm{ad}}-C_{44}{}^{\mathrm{iso}}=0.$$

The third term in the expression (6) for the elastic constants is particularly of interest. The summation is over all the different pairs of normal modes with a particular wave vector and belonging to different branches of the dispersion relations. Figure 11 shows the longitudinal-acoustic and transverse-optic dispersion curves at 296°K and at 90°K. At the higher temperature the curves are well separated, but at 90°K they appear to be almost degenerate over a considerable region of wave-vector space. Since at zero wave vector the temperature dependence of the transverse optic mode is given by Eq. (5), it might be expected that the temperature dependence of the denominator in the third term of Eq. (6) for these two normal modes is given by

$$\omega^2(\mathbf{q}j)-\omega^2(\mathbf{q}j') \quad \alpha \quad T-T_A,$$

[26] G. Leibfried and W. Ludwig, in *Solid State Physics*, edited by F. Seitz and D. Turnbull (Academic Press Inc., New York, 1961), Vol. 12.

where T_A is the temperature at which they become degenerate. The above temperature dependence can also be obtained by using a lowest order anharmonic theory of the temperature dependence of the normal modes.

The other factors in the expression for the elastic constants are either independent of temperature or as a first approximation can be written as proportional to temperature in a limited temperature range. The elastic constant is then given by an expression of the type

$$C_{\alpha\beta,\gamma\delta}=A+BT+C/(T-T_A). \quad (7)$$

The coefficients A, B, C can, in principle, be obtained from the matrix elements and summations over the normal modes. The coefficient C would be particularly difficult to evaluate, because it depends on the detailed shape of the dispersion curves near the degeneracy.

The temperature dependence of the elastic constants has been measured above 110°K by Bell and Rupprecht,[11] who obtained

$$\begin{aligned} C_{11}&=3.341\times10^{12}[1-2.62 \\ &\quad\times10^{-4}(T-T_A)-0.0992/(T-T_A)], \\ C_{12}&=1.049\times10^{12}[1-1.23 \\ &\quad\times10^{-4}(T-T_A)+0.1064/(T-T_A)], \quad (8) \\ C_{44}&=1.267\times10^{12}[1-1.30 \\ &\quad\times10^{-4}(T-T_A)-0.1242/(T-T_A)], \end{aligned}$$

with $T_A=108$°K.

These results are clearly in agreement with the temperature dependence predicted by Eq. (7). Bell and Rupprecht[11] also found that the ultrasonic attenuation increases dramatically near 110°K. The ultrasonic attenuation can be calculated in an exactly similar way to the elastic constant[27] and arises when the frequency Ω of the ultrasonic wave is such that

$$\Omega=\omega(\mathbf{q}j)-\omega(\mathbf{q}j'). \quad (9)$$

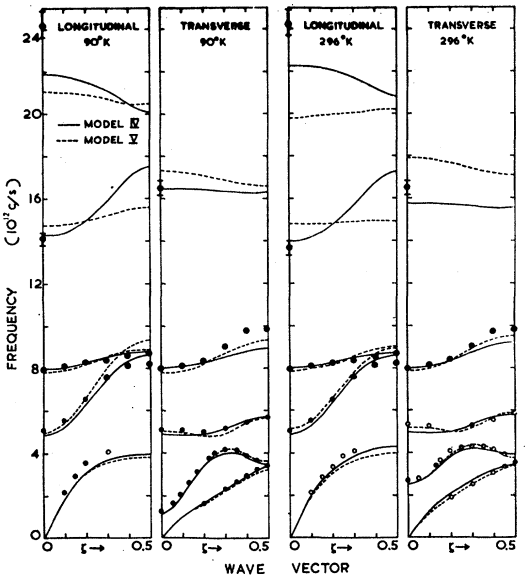

FIG. 9. The dispersion curves for model IV (solid line) and model V (dotted line) for normal modes propagating along the $(\zeta,0,0)$ direction. The experimental measurements are taken from both neutron and infrared spectrometry. (See Refs. 3 and 4.) The irreducible representations at the zone boundaries are for the longitudinal modes M_2', M_1, M_3, M_1, M_2' except for model V at 90°K which gives M_2', M_3, M_1, M_1, M_2' while for the transverse modes they are M_5, M_5', M_5, M_5', M_5. The irreducible representations are listed in order of increasing frequency.

If the transverse optic mode is almost degenerate with the longitudinal acoustic mode in this temperature region over a considerable region of $\mathbf{q}$ space, as suggested by Fig. 11, then there will be many normal modes for which Eq. (9) can be satisfied and the ultrasonic attenuation will be large.

2. The Transition

The elastic constants of the crystal will become negative just above T_A, Eqs. (8). When the elastic constants

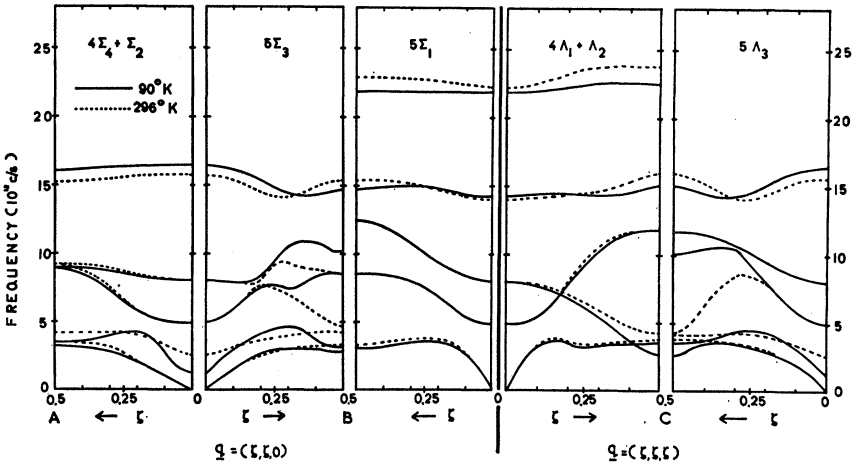

FIG. 10. The dispersion curves of model IV in the $(\zeta,\zeta,0)$ and (ζ,ζ,ζ) directions. In order of increasing frequency the irreducible representations are for the zone boundary (A) M_3', M_2', M_5, M_3' (90°K) and M_2', M_3', M_5, M_3' (296°K), for the zone boundary (B) M_3, M_5', M_5', M_2, M_1, M_5', M_4 (90°K) and M_5', M_3, M_2, M_5', M_1, M_5', M_4, while for the zone boundary (C) they are Γ_{25}, Γ_{15}, Γ_{12}', Γ_{15}, Γ_{25}', Γ_2' (90°K) and Γ_{15}, Γ_{25}, Γ_{12}', Γ_{15}, Γ_{25}', Γ_2' (296°K).

[27] R. A. Cowley, Advan. Phys. 12, 421 (1963).

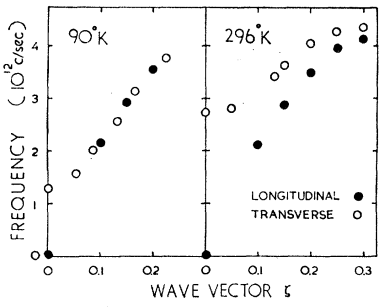

FIG. 11. The longitudinal acoustic and lowest transverse optical branches at 90 and 296°K.

become zero the crystal will undergo a spontaneous deformation to a new structure, the extent of the deformation depending upon the third- and fourth-order elastic constants. Since the elastic constant C_{44} becomes negative at the highest temperature, a tetragonal low-temperature structure can result by combining three shear distortions along different axes in the crystal. A tetragonal structure of strontium titanate below 110°K has been found by Rimai and deMars.[28] In this transition the volume of the crystal does not change, and it is extremely likely that the crystal splits up into small domains, with the major tetrad axis, the z direction in the domain, along different cube axes.

The elastic constants and the free energy of the crystal depend not only on the frequencies $\omega(\mathbf{q}j)$ and $\omega(\mathbf{q}j')$ which are nearly degenerate, but also on the number of these normal modes which are nearly degenerate. The temperature dependence of the distortion can then be estimated if we assume that its magnitude is proportional to the difference in the number of normal modes just above the degenerate frequency to those just below this. The frequencies squared of the transverse optic modes are linearly temperature-dependent, while the deformation is limited by the third-order elastic constants which are assumed to be independent of temperature. The temperature dependence of the distortion is then proportional to $(T_A-T)^{1/2}$ as found experimentally by Rimai and deMars.[28]

The discussion given above is very crude and cannot be expected to give satisfactory results at temperatures far away from the transition temperature. In particular the temperature dependence will depend on the effect of the distortion on the other normal modes, particularly near the degeneracy in the longitudinal acoustic and transverse optical branches, the temperature dependence of the population factors of the normal modes, and the effect of the domain structure on the free energy.

Below the transition the behavior of the elastic constants and ultrasonic attenuation will be very complex. The elastic constants will be an average over the different orientations of the domains, as well as being strongly affected by the exact details of the degeneracies of the normal modes and their behavior in the distorted crystal. The ultrasonic attenuation will also be anomalous because of reflection of the ultrasonic waves at the surfaces of the domains, as suggested by Bell and Rupprecht.[11]

[28] L. Rimai and G. A. deMars, Phys. Rev. **123**, 702 (1962).

3. The Dielectric Properties

Below 110°K the frequencies of the normal modes of vibration will be altered by the distortion of the crystal. It is likely that the frequency of the transverse optic mode will be particularly sensitive because of the large changes which occurred when small changes were made in the parameters of the models of Sec. IV. If the lattice spacing decreases by δa along the x and y directions and increases by $2\delta a$ along the unique z axis, the frequency of a transverse optical mode depends upon whether it is polarized along or perpendicular to the z axis.

The changes in the frequencies due to the distortion can be estimated from the volume dependence of the frequencies in the cubic structure. Equation (5) for the frequency will be modified to

$$\omega_z^2=K(T-T_c)+2\delta aB,$$
$$\omega_x^2=K(T-T_c)-\delta aB,$$

where ω_z is the normal mode polarized along the z axis and $B=d\omega^2/da$.

The distortion of the crystal then changes the Curie temperature by $-2\delta aB/K$ for displacements along the z axis, and by $\delta aB/K$ for those perpendicular to it.

The dielectric constant of a large crystal can then be estimated by assuming that there are an equal number of domains orientated with the z axis along each of the three original cube axes. The average dielectric constant is then

$$\frac{1}{\epsilon^0}=\frac{1}{3}\left(\frac{T-T_c+(2\delta aB/K)}{C}+2\frac{T-T_c-(\delta aB/K)}{C}\right),$$

and therefore,

$$\epsilon^0=C/(T-T_c).$$

The dielectric constant of a bulk sample of the distorted crystal is then identical with that of the crystal if there was no distortion. This result explains the rather surprising experimental result[11,22,23] that the reciprocal of the dielectric constant does not even change slope through the 110°K transition.

The distortion does however influence the low-temperature dielectric properties. Since the Curie temperature is raised in one direction, some of the domains can become polarized above T_c. This spontaneous polarization will occur along different directions in the crystal, corresponding to the different orientations of the domains, and will be frozen in to a particular configuration by the domain pattern produced by the 110°K transition.

The dielectric behavior at low temperatures will therefore be extremely complicated. Deviations from the Curie law will be caused by the spontaneous

polarization of some of the domains. Further and probably larger deviations will be caused by quantum effects. Barrett[29] demonstrated how these occur by using a Slater model of a ferroelectric, and very similar conclusions can be obtained by using a lattice dynamical approach. These two effects can probably account for the deviations from a Curie law found experimentally.[22,23]

When an electric field is applied the crystal shows a remanence polarization[22] at temperatures above 50°K, the size of this remanence polarization increasing as the temperature decreases. This polarization may be produced by the electric field aligning the spontaneous polarization of some of the domains, which is then frozen in by the domain structure when the field is released. The increase in magnitude with decreasing temperature arises because more and more domains become spontaneously polarized. The distortion required to shift the Curie temperature to 50°K, an increase of about 15°K, can be estimated from the measurements of the pressure dependence of the Curie temperature,[30] while the sign of the distortion is given by the change in free energy of the crystal. The change in the vibrational part of the free energy due to the changes in the frequency of the transverse optic mode show that the domains are probably elongated along the unique z axis. The dependence of the Curie temperature on lattice spacing is

$$\frac{dT_c}{da}=\frac{1.2\times10^4}{a}.$$

For an increase in Curie temperature of 15°K, the increase in length along the tetragonal axis is 0.005 Å, while the contraction perpendicular to the axis is 0.0025 Å. These distortions are very small, and could easily have been missed in the x-ray diffraction work quoted by Bell and Rupprecht.[11]

VI. DISCUSSION

1. The Parameters of the Models

The parameters for the rigid-ion model (I) show that both the short-range forces between the titanium and oxygen ions and the titanium and oxygen ionic charges are considerably smaller than for the shell models. This decrease in magnitude must in some way compensate for the neglect of the polarizabilities of the ions.

The parameters of all of the shell models are far more similar to one another than they are to the rigid-ion models. The parameters specifying the short-range forces in models II and III, in which the ionic charges were kept fixed, are very similar, but when the ionic charges were allowed to vary in models IV and V there was a decrease in the strontium-oxygen forces and a slight increase in the titanium-oxygen forces. These changes are accompanied by a decrease in the ionic charge of the strontium ions and an increase of the charge on the titanium ions.

It is of interest to compare the parameters of the short-range forces with those obtained by the method suggested by Fowler.[31] Devonshire,[32] Kinase,[33] and Dvorak and Janovec[34] have used these forces to describe the forces in perovskite ferroelectrics. In the notation of Sec. II.2, the parameters of their forces are:

$$A_1=30.1 \quad A_2=429.1 \quad A_3=63.5$$
$$B_1=-2.74 \quad B_2=-41.53 \quad B_3=-6.16.$$

Although these force constants are significantly different from those of any of the models of Sec. IV, they do exhibit some of the principal features; for example, A_2 is by far the largest. Nevertheless, the frequencies of the normal modes of vibration are so sensitive to small changes in the parameters that these short-range force constants do not give an adequate description of the interactions.

When the ionic charges were allowed to vary in the shell models (IV, V), the charge on the titanium ion becomes larger than four, and on the strontium ion about one electronic charge. The charge on the oxygen ions remains at nearly two. These results suggest that the bonding in strontium titanate is more nearly ionic than covalent in character.

There is a considerable reduction in the error of the models when the short-range polarizabilities of the positive ions are allowed to vary (III, IV). These polarizabilities of the positive ions come out either very small or negative, and cannot be readily understood in terms of the shell model. These results are exactly similar to those found for the alkali halides, potassium bromide and sodium iodide.[15] In an exactly analogous way to the alkali halides, when the titanium ion's electrical polarizability was allowed to vary (V) the polarizability of the positive ion was larger than the crystal polarizability,[35] while the polarizability of the oxygen ions was reduced. It was shown[15] that these surprising polarizability parameters could arise in the alkali halides from the neglect of the quadrupole moments produced on the negative ions. A similar explanation can be advanced here in terms of the quadrupole moments of the oxygen ions.

A surprising feature of the polarizabilities of the oxygen ions is their anisotropy. For example, the electrical polarizability of the oxygen ions for the 90°K model V is $2\frac{1}{2}$ times as large in the strontium-oxygen plane as in the titanium-oxygen direction. The short-range polarizability in the titanium-oxygen direction is -1.41, while it is 0.615 in the strontium-oxygen plane.

[29] J. H. Barrett, Phys. Rev. **86**, 118 (1952).
[30] W. J. Merz, Phys. Rev. **77**, 52 (1950).
[31] R. H. Fowler, *Statistical Mechanics* (Cambridge University Press, Cambridge, 1936), 2nd ed.
[32] A. F. Devonshire, Phil. Mag. **40**, 1040 (1949).
[33] W. Kinase, Progr. Theoret. Phys. (Kyoto) **13**, 529 (1955).
[34] V. Dvorak and V. Janovec, Czech. J. Phys. **812**, 461 (1962).
[35] J. R. Tessmann, A. H. Kahn, and W. Shockley, Phys. Rev. **92**, 890 (1953).

These polarizability parameters suggest that the electronic wave functions of the oxygen ions may be considerably distorted from spherical, and that the shell parameters Y_3 and k_3, which were assumed to be isotropic, should be different for different directions.

2. The Motion of the Ions in the Normal Modes

There has been considerable discussion as to the nature of the ionic displacements in the transverse optic modes of strontium titanate. The polarization vectors for these normal modes have been obtained for several of the models described earlier, and are listed in Table IV for model IV. The lowest frequency transverse optic mode is found to be predominantly a vibration of the titanium ion against the rest of the structure.

If the crystal becomes unstable against the lowest frequency transverse optic mode of vibration, it might be expected that the displacements of the ions would resemble the pattern of the displacements in the transverse optic mode of vibration.[2] It is therefore of interest to compare the displacements of the ions with the measured displacements of the ions in tetragonal barium titanate,[36] and these are also shown in Table IV. Considering the difference in the masses, sizes and polarizabilities of strontium and barium ions, the displacements of the ions in barium titanate are fairly similar to those in the lowest transverse optic mode of strontium titanate.

3. The Temperature Dependence of the Transverse Optic Modes

One of the most interesting features of strontium titanate is the temperature dependence of the transverse optic mode of lowest frequency. The difference between the parameters of the models which were fitted to the measurements at 90°K and those fitted to the 296°K measurements are not large, and model VI shows that it is possible to obtain the temperature dependence by changing the parameters of the short-range interactions by quite small amounts. These results show that only quite small changes in the parameters of the interactions can give rise to the observed temperature dependence.

The temperature dependence of the normal modes in potassium bromide has been investigated both experimentally[10] and theoretically.[15] The changes in the parameters of the models, which are needed to reproduce the changes in the frequencies of the normal modes from 90 to 400°K, are fractionally very similar to those required for strontium titanate. We can therefore conclude that, broadly speaking, it is not necessary to invoke any mechanism to explain the temperature dependence in strontium titanate, other than what is present in the alkali halides.

The temperature dependence of the normal modes in sodium iodide and potassium bromide has recently been shown to arise largely from the anharmonic interactions between the normal modes.[37] Quantitative calculations of the anharmonic effects in strontium titanate, which will be reported elsewhere, suggest that a similar mechanism is responsible for the temperature dependence of its normal modes.

The anomalous behavior of the normal modes in strontium titanate compared with the alkali halides is associated with the difference in the dynamical matrices of the two crystals. In the alkali halides, the frequencies of the normal modes are all fairly similar in magnitude (apart from the elastic constants region of the acoustic branches). For strontium titanate, on the other hand, there is a very large difference between the frequencies of the optical modes. At 90°K the ratio of the highest to lowest eigenvalue (frequency squared) of the dynamical matrix is as large as 400:1. A change in the parameters of only 0.25% will then hardly alter the largest eigenvalue but can drastically alter the smallest. The ferroelectric character of these perovskites then arises from the almost perfect cancellation of the strong short-range and Coulomb interactions for one particular normal mode. A small change in either of these strong interactions has a drastic effect on the frequencies of this normal mode.

TABLE IV. The displacements of the ions in the $\mathbf{q}=0$ modes of model IV at 90°K, polarized along the z direction, and expressed so that the eigenvectors of the dynamical matrix are normalized and orthogonal. The numbering of the modes is in order of increasing frequency.

Model IV	Ti	Sr	O_{III}	O_I	O_{II}
Transverse					
(1)	0.077	0.022	−0.093	−0.129	−0.129
(2)	0.097	−0.074	0.035	0.040	0.040
(3)	0	0	0	−0.177	0.177
(4)	0.007	0.004	−0.217	0.087	0.087
Longitudinal					
(1)	0.080	−0.077	0.050	0.065	0.065
(2)	0	0	0	−0.177	0.177
(3)	0.057	0.001	0.107	−0.143	−0.143
(4)	0.075	0.008	−0.207	−0.032	−0.032
Displacements of ions in $BaTiO_3$ transition[a] (Å)	0.053	0.003	−0.051	−0.047	−0.047

[a] See Ref. 36.

4. Unstable Normal Modes in the (1,1,0) and (1,1,1) Directions

Several of the models described in Sec. IV show instabilities against some of the normal modes of vibration propagating along the (1,1,0) and (1,1,1) directions. Examples of these are shown in Fig. 8 for models III and V. It is unlikely that these instabilities occur in strontium titanate and in this respect those models

[36] B. C. Frazer, H. R. Danner, and R. Pepinsky, Phys. Rev. **100**, 745 (1955).

[37] R. A. Cowley, Phys. Chem. Solids (to be published).

which show them are unrealistic. However, these instabilities may well occur in some of the perovskite materials which have phases that are slightly distorted forms of the cubic perovskite structure. For example, $CdTiO_3$, $NaTaO_3$, $CaTiO_3$, $NaNbO_3$ show multiple unit cells which are $2\times2\times2$ times the cubic cell when referred to the original cube axes while $NaNbO_3$ shows a $4\times2\times2$ unit cell, and $PbZrO_3$ shows a $4\times4\times2$ unit cell.[38]

All of the unstable normal modes are rotations of groups of the oxygen ions. In models I and V octahedra rotate around the titanium ion while in model III squares of oxygens rotate about the points $(\frac{1}{2},0,0)$, $(0,\frac{1}{2},0)$ and $(0,0,\frac{1}{2})$. A further feature of these unstable normal modes is that their frequencies are very dependent upon the details of the models. For example, the normal mode Γ_{25}' are unstable for models I and V but for model III have a frequency of 2.6 and for model IV of 3.5.

The transitions to the multiple unit cell perovskites may well be instabilities against these normal modes as suggested by Cochran.[2] Unfortunately the displacements of the ions in real distorted perovskite structures are far more complex than mere oxygen octahedra rotations. However, in several of these materials, the rotations of the oxygen octahedra are the predominant displacements.[39] The displacements of the other ions are not, however, negligible and a detailed treatment would be very complicated. The unstable normal mode must be strongly coupled both to the macroscopic strain parameters and to some of the other normal modes in the crystal.

5. The Models of Other Authors

Several authors have previously used models for the lattice dynamics of perovskite ferroelectrics. Devonshire[32] used a rigid-ion model with Fowler's[31] short-range forces to attempt to relate the parameters of his thermodynamic theory to the microscopic interactions. Recently Dvorak and Janovec[34] have calculated the frequencies of the transverse optic modes of this model, and have found the structure unstable unless the formal ionic charges are multiplied by a factor 0.16. The frequencies are not then in agreement with the results of neutron or infrared spectrometry.

Kinase[33] has used this model, and included the electrical polarizabilities of the ions, but the results were no more satisfactory.

Last[18] suggested that the infrared spectra could be explained by assuming that the titanium-oxygen octahedra was a strongly bound complex which was weakly coupled to the other anion. As the lowest frequency optic mode is a vibration of the titanium against the rest of the structure this model is unsatisfactory. Rajopal and Srinivasan[40] studied the frequencies of vibration at $\mathbf{q}=0$ when all the Coulomb forces are neglected. The high- and low-frequency dielectric constants of this model are then equal (to unity!) and the frequencies do not agree with the experimental results. A similar model has been used by Silverman and Joseph[41] for the transverse optic modes with $\mathbf{q}=0$.

VII. CONCLUSIONS

The frequency versus wave-vector dispersion curves of strontium titanate for several normal modes propagating in the [0,0,1] direction have been measured experimentally by using neutron spectrometry. These results have been used to find the parameters of several models of the crystal within the harmonic approximation. It was found that quite reasonable agreement with experiment could be obtained by using shell models in which the ions interact with one another both through short-range forces between neighboring ions, and through long-range electrostatic forces, determined by the ionic charges. The effects of the polarizabilities of the ions are also included. The principal features of the more successful models are that the titanium-oxygen short-range forces are very large, while the ionic charges on the ions are also large and very nearly the formal charges.

Of particular interest in strontium titanate is the temperature dependence of the transverse optic mode with lowest frequency. This was measured experimentally and for the $\mathbf{q}=0$ mode the square of the frequency was found to be proportional to temperature above 90°K, in agreement with the temperature dependence of the static dielectric constant as predicted by Cochran.[2] This result shows that it is a valid approach to treat the problem of ferroelectricity as an instability of the crystal against one of the normal modes. The motion of the ions in this normal mode was obtained for several of the models used, and was found to be predominantly a vibration of the titanium ion against the oxygen octahedron. The displacements of the ions at the ferroelectric transition in barium titanate are very similar to this.

It was found that the experimentally observed changes in the frequencies of this normal mode could be obtained by changing the parameters of the shell models only slightly. The fractional changes were very similar to those needed to reproduce the temperature dependence of the normal modes in the alkali halides. This result suggests that it is unnecessary to introduce any mechanism to explain the temperature dependence of this normal mode, other than those which occur in the alkali halides. The indications are then that the temperature dependence of this normal mode can be explained

[38] F. Jona and G. Shirane, *Ferroelectric Crystals* (Pergamon Press, Inc., New York, 1963).
[39] H. D. Megaw, *Ferroelectricity in Crystals* (Methuen and Company, Ltd., London, 1957).
[40] R. K. Rajopal and R. Srinivasan, Phys. Chem. Solids **23**, 633 (1962).
[41] B. D. Silverman and R. I. Joseph, Technical Memorandum T-451, Raytheon Company, 1963 (unpublished).

in terms of the anharmonic interactions between the normal modes of vibration.

The dispersion curves along the (1,1,0) and (1,1,1) directions of the models have been calculated and some of these show normal modes against which the crystal would be unstable. Although it is unlikely that these instabilities occur in strontium titanate, they may well be associated with the transitions in other perovskite materials.

The transition in strontium titanate at 110°K has been discussed in terms of an accidental degeneracy of two branches of the dispersion curves. The experimental results from neutron spectrometry show that this degeneracy occurs very near 110°K. The anomalous elastic properties near 110°K and the smooth behavior of the static dielectric constant can be easily obtained with this theory. It is suggested that the conflicting experimental results on the low-temperature dielectric properties, and the temperature dependence of the distortion of the crystal can also be explained by this approach.

It is clearly of interest to try to obtain more satisfactory models of strontium titanate, in the hope of obtaining a better understanding of both the temperature dependence of the static dielectric constant and of the 110°K transition. Experimental measurements of the dispersion curves in the (1,1,0) and (1,1,1) directions would enable the parameters of the models to be fitted more accurately. The models could then be extended by including anisotropic oxygen polarizabilities, more short-range forces, and abandoning the assumption that $\mathbf{R}=\mathbf{T}=\mathbf{S}$.

The difficulties in describing the results in terms of a harmonic model might then become more serious, and it might well prove necessary to use a complete anharmonic theory to describe the lattice vibrations.

ACKNOWLEDGMENTS

The author is grateful for helpful discussions on the experimental measurements with Professor B. N. Brockhouse, on group theory with Dr. V. Heine, and on distorted perovskite structures with Dr. H. D. Megaw and Dr. I. Lefkowitz. Above all, however, he is indebted to Dr. W. Cochran, F.R.S., who suggested the study of strontium titanate and who has continually given helpful advice and criticism.

The author is grateful for the award of a NATO studentship from the Department of Scientific and Industrial Research and to Atomic Energy of Canada Ltd. for allowing him to use experimental facilities. Permission to use the EDSAC II computer at the Cambridge University Mathematical Laboratory was given by Dr. M. V. Wilkes, F.R.S., for which the author is grateful. The excellent single crystal of strontium titanate was provided by the Titanium Division of the National Lead Company, for which the author is grateful.

APPENDIX I

A. The Characters of the Symmetry Operations

The representation chosen for the normal modes is obtained by displacing each ion in turn along the coordinate axes by a unit distance. The characters of the different symmetry elements are:

identity operator

$$\chi(E)=15,$$

triad axis

$$\chi(C_3)=0,$$

tetrad axis along the z axis

$$\chi(C_{4z})=1+2\exp(i2q_xr),$$

diad axis along the z axis

$$\chi(C_{2z})=-1-\exp(i2q_xr)-\exp(i2q_yr)-2\exp(i2(q_x+q_y)r),$$

diad axis at 45° to both x and y axes

$$\chi(C_{2xy}')=-2-\exp(i2q_zr),$$

inversion operator

$$\chi(I)=-3[1+\exp(i2(q_x+q_y+q_z)r)+\exp(i2(q_x+q_y)r)+\exp(i2(q_y+q_z)r)+\exp(i2(q_x+q_z)r)],$$

plane of symmetry perpendicular to the z axis

$$\chi(\sigma_{xy})=2+3\exp(i2q_zr),$$

plane of symmetry at 45° to x and y axes and including z axis

$$\chi(\sigma_d)=3,$$

inversion tetrad axis along the z axis

$$\chi(S_{4z})=-1-\exp(i2q_xr)-\exp(i2(q_x+q_z)r),$$

inversion hexad axis

$$\chi(S_6)=0.$$

B. The Displacements of the Ions in Different Normal Modes

Irreducible representation	Normal mode
$\zeta=(0,0,\zeta)$	
Δ_1	Sr_z, Ti_z, O_{Iz}, $O_{IIz}=O_{IIIz}$.
Δ_2	$O_{IIz}=-O_{IIIz}$.
Δ_5	Sr_x, Ti_xO_{Ix}, O_{IIx}, O_{IIIx}. Sr_y, Ti_y, O_{Iy}, O_{IIy}, O_{IIIy}.
$\zeta=(0,0,\frac{1}{2})$	
M_1	Ti_z, $O_{IIz}=O_{IIIz}$.
M_2'	Sr_z, O_{Iz}.
M_3	$O_{IIz}=-O_{IIIz}$.
M_5	Ti_x, O_{IIx}, O_{IIIx}. Ti_y, O_{IIy}, O_{IIIy}.
M_5'	Sr_x, O_{Ix}. Sr_y, O_{Iy}.
$\zeta=(\zeta,\zeta,0)$	
Σ_1	$Ti_x=Ti_y$, $Sr_x=Sr_y$, $O_{Ix}=O_{Iy}$, $O_{IIx}=O_{IIIy}$, $O_{IIIx}=O_{IIy}$.
Σ_2	$O_{IIz}=-O_{IIIz}$.
Σ_3	$Ti_x=-Ti_y$, $Sr_x=-Sr_y$, $O_{Ix}=-O_{Iy}$, $O_{IIx}=-O_{IIIy}$, $O_{IIIx}=-O_{IIy}$.
Σ_4	Ti_z, Sr_z, O_{Iz}, $O_{IIz}=O_{IIIz}$.
$\zeta=(\frac{1}{2},\frac{1}{2},0)$	
M_1	$O_{IIx}=O_{IIIy}$.
M_2	$O_{IIIx}=-O_{IIy}$.
M_3	$O_{IIx}=-O_{IIIy}$.
M_4	$O_{IIIx}=O_{IIy}$.
M_2'	Sr_z.
M_3'	Ti_z, O_{Iz}.
M_5	O_{IIz}. O_{IIIz}.
M_5'	Ti_x, Sr_y, O_{Ix}. Ti_y, Sr_x, O_{Iy}.
$\zeta=(\zeta,\zeta,\zeta)$	
Λ_1	$Sr_x=Sr_y=Sr_z$, $Ti_x=Ti_y=Ti_z$, $O_{IIIx}=O_{IIy}=O_{Iz}$, $O_{IIIy}=O_{IIIz}$ $=O_{IIx}=O_{IIz}=O_{Ix}=O_{Iy}$.
Λ_2	$O_{Ix}=O_{IIz}=O_{IIIy}=-O_{Iy}$ $=-O_{IIx}=-O_{IIIz}$.
Λ_3	$Ti_x=-(Ti_y+Ti_z)$, $Sr_x=-(Sr_y+Sr_z)$, $O_{IIIx}=-(O_{IIy}+O_{Iz})$, $O_{Ix}=-(O_{IIIy}+O_{IIz})$,
$\zeta=(\zeta,\zeta,\zeta)$	
Λ_3	$O_{IIx}=-(O_{Iy}+O_{IIIz})$. $Ti_z=-Ti_y$, $Sr_z=-Sr_y$, $O_{Iz}=-O_{IIy}$, O_{IIz} $=-O_{IIIy}$, $O_{IIIz}=-O_{Iy}$.
$\zeta=(\frac{1}{2},\frac{1}{2},\frac{1}{2})$	
Γ_2'	$O_{Iz}=O_{IIy}=O_{IIIx}$.
Γ_{12}'	$O_{Iz}=O_{IIy}=-\frac{1}{2}O_{IIIx}$. $O_{Iz}=-O_{IIy}$.
Γ_{25}	$O_{Iy}=-O_{IIz}$. $O_{Ix}=-O_{IIIz}$. $O_{IIx}=-O_{IIIy}$.
Γ_{25}'	Ti_x. Ti_y. Ti_z.
Γ_{15}	Sr_x, $O_{Iy}=O_{IIz}$. Sr_y, $O_{Ix}=O_{IIIz}$. Sr_z, $O_{IIx}=O_{IIIy}$.
$\zeta=(\frac{1}{2},\frac{1}{2},\zeta)$	
Δ_1	Sr_z, $O_{IIx}=O_{IIIy}$.
Δ_1'	$O_{IIIx}=-O_{IIy}$.
Δ_2	$O_{IIx}=-O_{IIIy}$.
Δ_2'	Ti_z, $O_{IIIx}=O_{IIy}$, O_{Iz}.
Δ_5	Ti_x, Sr_y, O_{Ix}, O_{IIIz}. Ti_y, Sr_x, O_{Iy}, O_{IIz}.
$\zeta=(\zeta,\zeta,\frac{1}{2})$	
Σ_1	Ti_z, $Sr_x=Sr_y$, $O_{IIIz}=O_{IIz}$, $O_{Iy}=O_{Ix}$.
Σ_3	$Sr_x=-Sr_y$, $O_{IIIz}=-O_{IIz}$, $O_{Iy}=-O_{Ix}$.
Σ_4	$Ti_x=Ti_y$, Sr_z, O_{Iz}, $O_{IIy}=O_{IIIx}$, $O_{IIx}=O_{IIIy}$.
Σ_2	$Ti_x=-Ti_y$, $O_{IIIx}=-O_{IIy}$, $O_{IIx}=-O_{IIIy}$.
$\zeta=(\frac{1}{2},0,\zeta)$	
Σ_1	Ti_x, Sr_z, O_{Ix}, O_{IIx}, O_{IIIz}.
Σ_4	Sr_y, O_{IIIy}.
Σ_3	Ti_z, Sr_x, O_{IIIx}, O_{IIz}, O_{Iz}.
Σ_2	Ti_y, O_{Iy}, O_{IIy}.

C. The Compatibility Relations

$\zeta=(0,0,\zeta)$ with $\zeta=(0,0,0)$:

$\Gamma_{15}-\Delta_2+\Delta_5$, $\Gamma_{25}-\Delta_2+\Delta_5$.

$\zeta=(0,0,\zeta)$ with $\zeta=(0,0,\frac{1}{2})$:

Δ_1-M_1, Δ_1-M_2', Δ_2-M_3, Δ_5-M_5, Δ_5-M_5'.

$\zeta=(\zeta,\zeta,0)$ with $\zeta=(0,0,0)$:

$\Gamma_{15}-\Sigma_1+\Sigma_3+\Sigma_4$, $\Gamma_{25}-\Sigma_1+\Sigma_3+\Sigma_2$.

$\zeta=(\zeta,\zeta,0)$ with $\zeta=(\frac{1}{2},\frac{1}{2},0)$:

$M_1-\Sigma_1$, $M_2-\Sigma_3$, $M_2'-\Sigma_4$, $M_3-\Sigma_3$, $M_3'-\Sigma_4$, $M_4-\Sigma_1$, $M_5-\Sigma_2+\Sigma_4$, $M_5'-\Sigma_1+\Sigma_3$.

$\zeta=(\zeta,\zeta,\zeta)$ with $\zeta=(0,0,0)$:

$\Gamma_{15}-\Lambda_1+\Lambda_3$, $\Gamma_{25}-\Lambda_2+\Lambda_3$.

$\zeta=(\zeta,\zeta,\zeta)$ with $\zeta=(\frac{1}{2},\frac{1}{2},\frac{1}{2})$:

$\Gamma_{25}'-\Lambda_1+\Lambda_3$, $\Gamma_{15}-\Lambda_1+\Lambda_3$, $\Gamma_{25}-\Lambda_2+\Lambda_3$, $\Gamma_2'-\Lambda_1$, $\Gamma_{12}'-\Lambda_3$.

$\zeta=(\frac{1}{2},\frac{1}{2},\zeta)$ with $\zeta=(\frac{1}{2},\frac{1}{2},0)$:

$M_1-\Delta_1$, $M_2-\Delta_1'$, $M_2'-\Delta_1$, $M_3-\Delta_2$, $M_3'-\Delta_2'$, $M_4-\Delta_2'$, $M_5-\Delta_5$, $M_5'-\Delta_5$.

$\zeta=(\frac{1}{2},\frac{1}{2},\zeta)$ with $\zeta=(\frac{1}{2},\frac{1}{2},\frac{1}{2})$:

$\Gamma_2'-\Delta_2'$, $\Gamma_{12}'-\Delta_1'+\Delta_2'$, $\Gamma_{25}-\Delta_2+\Delta_5$, $\Gamma_{15}-\Delta_1+\Delta_5$, $\Gamma_{25}'-\Delta_2'+\Delta_5$.

$\zeta=(\zeta,\zeta,\frac{1}{2})$ with $\zeta=(0,0,\frac{1}{2})$:

$M_1-\Sigma_1$, $M_2'-\Sigma_4$, $M_3-\Sigma_3$, $M_5-\Sigma_2+\Sigma_4$, $M_5'-\Sigma_1+\Sigma_3$.

$\zeta=(\zeta,\zeta,\frac{1}{2})$ with $\zeta=(\frac{1}{2},\frac{1}{2},\frac{1}{2})$:

$\Gamma_2'-\Sigma_4$, $\Gamma_{12}'-\Sigma_2+\Sigma_4$, $\Gamma_{25}-\Sigma_1+\Sigma_2+\Sigma_3$, $\Gamma_{15}-\Sigma_1+\Sigma_3+\Sigma_4$, $\Gamma_{25}'-\Sigma_1+\Sigma_2+\Sigma_4$.

$\zeta=(\frac{1}{2},0,\zeta)$ with $\zeta=(\frac{1}{2},0,0)$:

$M_1-\Sigma_1$, $M_2'-\Sigma_3$, $M_3-\Sigma_1$, $M_5-\Sigma_2+\Sigma_3$, $M_5'-\Sigma_4+\Sigma_1$.

$\zeta=(\frac{1}{2},0,\zeta)$ with $\zeta=(\frac{1}{2},0,\frac{1}{2})$:

$M_1-\Sigma_1$, $M_2-\Sigma_3$, $M_2'-\Sigma_4$, $M_3-\Sigma_1$, $M_3'-\Sigma_2$, $M_4-\Sigma_3$, $M_5-\Sigma_2+\Sigma_4$, $M_5'-\Sigma_1+\Sigma_3$.

APPENDIX II: THE CONTRIBUTION OF THE SHORT-RANGE FORCES TO THE MATRIX $R(KK')$

The complete (15×15) matrix can be split up into the (5×5) matrices for the (xx), $(yy)\cdots$ components. In this appendix the (xx) and (xy) components are tabulated, in terms of the force constants introduced in Sec. II.2. C_x, C_y, C_z are the cosines of $q_x r$, $q_y r$, $q_z r$, while S_x, S_y, S_z are the analogous sines, and $2r$ is the lattice parameter.

The matrix $\mathbf{R}_{xx}$ in units of e^2/v is

	Ti	Sr	O_I	O_{II}	O_{III}
Ti	A_2+2B_2	0	$-B_2C_z$	$-B_2C_y$	$-A_2C_x$
Sr	0	$2A_1+4B_1$	$-(A_1+B_1)C_xC_y$	$-(A_1+B_1)C_xC_z$	$-2B_1C_yC_z$
O_I	$-B_2C_z$	$-(A_1+B_1)C_xC_y$	$A_1+B_1+B_2+A_3+3B_3$	$-2B_3C_yC_z$	$-(A_3+B_3)C_xC_z$
O_{II}	$-B_2C_y$	$-(A_1+B_1)C_xC_z$	$-2B_3C_yC_z$	$A_1+B_1+B_2+A_3+3B_3$	$-(A_3+B_3)C_xC_y$
O_{III}	$-A_2C_x$	$-2B_1C_yC_z$	$-(A_3+B_3)C_xC_z$	$-(A_3+B_3)C_xC_y$	$2B_1+A_2+2A_3+2B_3$

The matrix $\mathbf{R}_{xy}$ is, in units e^2/v:

	Ti	Sr	O_I	O_{II}	O_{III}
Ti	0	0	0	0	0
Sr	0	0	$(A_1-B_1)S_xS_y$	0	0
O_I	0	$(A_1-B_1)S_xS_y$	0	0	0
O_{II}	0	0	0	0	$(A_3-B_3)S_xS_y$
O_{III}	0	0	0	$(A_3-B_3)S_xS_y$	0

APPENDIX III

TABLE V. Coulomb coefficients.[a]

$\zeta = (0,0,\zeta)$

Ti-Ti

ζ	xx	yy	zz
0.5	−4.844	−4.844	9.687
0.4	−4.782	−4.782	9.563
0.3	−4.618	−4.618	9.236
0.2	−4.416	−4.416	8.832
0.1	−4.252	−4.252	8.503
0	−4.189	−4.189	8.378

Ti-Sr

ζ	xx	yy	zz
0.5	0	0	0
0.4	−1.281	−1.281	2.561
0.3	−2.443	−2.443	4.886
0.2	−3.375	−3.375	6.750
0.1	−3.979	−3.979	7.958
0	−4.189	−4.189	8.378

Ti-O$_\mathrm{I}$

ζ	xx	yy	zz
0.5	0	0	0
0.4	3.339	3.339	−6.678
0.3	6.359	6.359	−12.717
0.2	8.765	8.765	−17.530
0.1	10.316	10.316	−20.632
0	10.852	10.852	−21.704

Ti-O$_\mathrm{III}$

ζ	xx	yy	zz
0.5	−33.622	10.323	23.299
0.4	−33.684	10.373	23.311
0.3	−33.845	10.505	23.341
0.2	−34.046	10.668	23.377
0.1	−34.208	10.801	23.407
0	−34.271	10.852	23.419

Sr-O$_\mathrm{I}$

ζ	xx	yy	zz
0.5	−7.996	−7.996	15.992
0.4	−8.046	−8.046	16.091
0.3	−8.177	−8.177	16.354
0.2	−8.340	−8.340	16.679
0.1	−8.472	−8.472	16.944
0	−8.523	−8.523	17.045

Sr-O$_\mathrm{III}$

ζ	xx	yy	zz
0.5	0	0	0
0.4	1.370	−2.619	1.249
0.3	2.614	−4.989	2.376
0.2	3.610	−6.880	3.271
0.1	4.255	−8.101	3.846
0	4.479	−8.523	4.044

$\zeta = (\zeta,\zeta,0)$

Ti-Ti

ζ	xx	yy	zz	xy	yz	xz
0.5	2.677	2.677	−5.354	0	0	0
0.4	2.627	2.627	−5.255	0.716	0	0
0.3	2.492	2.492	−4.985	2.466	0	0
0.2	2.313	2.313	−4.626	4.394	0	0
0.1	2.157	2.157	−4.313	5.787	0	0
0	2.094	2.094	−4.189	6.283	0	0

Ti-Sr

ζ	xx	yy	zz	xy	yz	xz
0.5	0	0	0	10.620	0	0
0.4	0.196	0.196	−0.392	10.094	0	0
0.3	0.713	0.713	−1.426	8.841	0	0
0.2	1.360	1.360	−2.720	7.515	0	0
0.1	1.890	1.890	−3.780	6.599	0	0
0	2.094	2.094	−4.189	6.283	0	0

Ti-O$_\mathrm{I}$

ζ	xx	yy	zz	xy	yz	xz
0.5	16.559	16.559	−33.118	0	0	0
0.4	16.608	16.608	−33.215	0.702	0	0
0.3	16.741	16.741	−33.482	2.426	0	0
0.2	16.919	16.919	−33.838	4.353	0	0
0.1	17.074	17.074	−34.147	5.771	0	0
0	17.135	17.135	−34.271	6.283	0	0

Ti-O$_\mathrm{III}$

ζ	xx	yy	zz	xy	yz	xz
0.5	0	0	0	0	0	0
0.4	−9.436	6.240	3.196	2.003	0	0
0.3	−17.483	11.323	6.160	3.779	0	0
0.2	−23.351	14.732	8.618	5.147	0	0
0.1	−26.838	16.570	10.268	5.997	0	0
0	−27.988	17.135	10.852	6.283	0	0

Sr-O$_\mathrm{I}$

ζ	xx	yy	zz	xy	yz	xz
0.5	0	0	0	17.060	0	0
0.4	−0.210	−0.210	0.420	15.924	0	0
0.3	−0.763	−0.763	1.526	13.071	0	0
0.2	−1.455	−1.455	2.909	9.756	0	0
0.1	−2.021	−2.021	4.043	7.221	0	0
0	−2.239	−2.239	4.479	6.283	0	0

Sr-O$_\mathrm{III}$

ζ	xx	yy	zz	xy	yz	xz
0.5	0	0	0	0	0	0
0.4	4.013	−1.535	−2.477	1.852	0	0
0.3	7.221	−2.429	−4.792	3.568	0	0
0.2	9.316	−2.581	−6.734	4.991	0	0
0.1	10.423	−2.370	−8.053	5.946	0	0
0	10.762	−2.240	−8.523	6.283	0	0

$\zeta = (\zeta,\zeta,\zeta)$

Ti-Ti

ζ	xx	yy	zz	xy	yz	xz
0.5	0	0	0	0	0	0
0.4	0	0	0	0.283	0.283	0.283
0.3	0	0	0	1.170	1.170	1.170
0.2	0	0	0	2.499	2.499	2.499
0.1	0	0	0	3.706	3.706	3.706
0	0	0	0	4.189	4.189	4.189

Ti-Sr

ζ	xx	yy	zz	xy	yz	xz
0.5	0	0	0	0	0	0
0.4	0	0	0	2.923	2.923	2.923
0.3	0	0	0	4.655	4.655	4.655
0.2	0	0	0	4.934	4.934	4.934
0.1	0	0	0	4.472	4.472	4.472
0	0	0	0	4.189	4.189	4.189

Ti-O$_\mathrm{III}$

ζ	xx	yy	zz	xy	yz	xz
0.5	0	0	0	0	0	0
0.4	−9.860	4.930	4.930	1.121	0.151	1.121
0.3	−18.557	9.278	9.278	2.198	0.987	2.198
0.2	−25.047	12.524	12.524	3.178	2.404	3.178
0.1	−28.856	14.428	14.428	3.911	3.686	3.911
0	−30.082	15.041	15.041	4.189	4.189	4.189

Sr-O$_\mathrm{I}$

ζ	xx	yy	zz	xy	yz	xz
0.5	0	0	0	14.461	0	0
0.4	−0.553	−0.553	1.107	13.462	0.466	0.466
0.3	−1.858	−1.858	3.715	10.842	1.618	1.618
0.2	−3.189	−3.189	6.379	7.641	2.908	2.908
0.1	−4.052	−4.052	8.104	5.125	3.851	3.851
0	−4.334	−4.334	8.668	4.189	4.189	4.189

[a] The dimensionless Coulomb coefficients are defined in Ref. 16. If these numbers are multiplied by $(e^2/v)Z_\kappa Z_{\kappa'}$ they give the Coulomb contributions to the dynamical matrix.